의학석사 학위논문

PET imaging of dopamine transporters with [^{18}F]FE-PE2I: Effects of anti-parkinsonian drugs

항파킨슨병 약물이 도파민 운반체 PET 방사성 추적자 [^{18}F]FE-PE2I의 도파민 운반체 결합에 미치는 영향

2015년 7월

서울대학교 대학원

의학과 뇌신경과학 전공

방 지 인

PET imaging of dopamine transporters with [^{18}F]FE-PE2I: Effects of anti-parkinsonian drugs

항파킨슨병 약물이 도파민 운반체 PET 방사성 추적자 [^{18}F]FE-PE2I의 도파민 운반체 결합에 미치는 영향

지도교수 김 상 은

이 논문을 의학석사 학위논문으로 제출함

2015년 7월

서울대학교 대학원

의학과 뇌신경과학 전공

방 지 인

방지인의 석사학위논문을 인준함

2015년 7월

위 원 장 김 지 수 (인)

부위원장 김 상 은 (인)

위 원 이 원 우 (인)

Abstract

PET imaging of dopamine transporters with [^{18}F]FE-PE2I: Effects of anti-parkinsonian drugs

Ji-In Bang

College of Medicine, Department of Neuroscience

The Graduate School

Seoul National University

***Purpose*:**

[^{18}F]FE-PE2I is a promising radioligand for dopamine transporter (DAT) imaging. This study aimed to determine any correlation between striatal [^{18}F]FE-PE2I binding and immunohistochemical (IHC) stain of tyrosine hydroxylase (TH) in the striatum, and to evaluate the effects of therapeutic drugs on [^{18}F]FE-PE2I binding.

Materials and Methods:

Dynamic PET/CT of [^{18}F]FE-PE2I was performed on Parkinson's diease (PD) rat models, induced by unilateral injection of 6-OHDA into the striatum. A simplified reference tissue model using the cerebellum as a reference was used to calculate the striatal binding potential (striatal BP_{ND}). Ratio of optical density (OD) of TH-reactive fibers in the PD and normal rats was correlated with ratio of striatal BP_{ND}. To study therapeutic drug effects, each of the 4 normal rats were pretreated with L-DOPA combined with benserazide, pramipexole, amantadine and escitalopram 30 min before [^{18}F]FE-PE2I injection. The L-DOPA/benserazide effect on lesioned and unlesioned striatal BP_{ND} was also assessed in the PD rats.

Results*:*

The BP_{ND} was significantly lower in the lesioned striatum than in the unlesioned one or the striatum of normal rats. The ratio of OD of TH-reactive fibers linearly correlated with the ratio of striatal BP_{ND} ($r=0.741$, $P<0.05$). After the pre-treatment with pramipexole, amantadine and escitalopram, the values of striatal BP_{ND} did not differ from those of control rats. However, pre-treatment of L-DOPA/benserazide significantly reduced the striatal BP_{ND} ($P=0.03$). The striatal BP_{ND} of PD rats with L-DOPA/benserazide was not different from those of same PD rats with placebo (normal saline) treatment. For midbrain binding, pretreatment of escitalopram did not affect the midbrain BP_{ND} on normal rats.

Conclusion:

[^{18}F]FE-PE2I may be used as a radioligand for in vivo imaging of the DAT. In normal rats, [^{18}F]FE-PE2I binding is unaffected by therapeutic drugs for PD including pramipexole, amantadine and escitalopram. L-DOPA/benserazide does not affect the striatal [^{18}F]FE-PE2I binding in PD rats.

Key words: Parkinson disease (PD); Dopamine transporter (DAT); (E)-N-(3-iodoprop-2-enyl)-2beta-carbofluoroethoxy-3beta-(4'-methyl-phenyl) nortropane; Levodopa; Positron-Emission Tomography (PET)

Student Number: 2013-23506

List of Figures

Contents

Introduction

Dopamine transporter (DAT) is a presynaptic transmembrane protein that regulates the dopamine (DA) concentration in the synapse (1). Changes in the density and function of DAT have been reported in various neuropsychiatric disorders, such as Parkinson's disease (PD), Huntington's disease, schizophrenia, and ADHD (2-5). Molecular imaging is an established tool for the evaluation of DAT in vivo and assessment of the pathophysiology of such diseases.

Among the various DAT imaging radioligands for both single-photon emission computed tomography (SPECT) and positron emission tomography (PET) imaging, N-(3-iodoprop-2-enyl)-2β-carbomethoxy-3β-(4-methylphenyl)nortropane (PE2I) demonstrated a high affinity for DAT and selectivity for DAT over the norepinephrine and serotonin transporter (SERT) (6, 7). Several animal models and human studies have been performed with ^{11}C labeled PE2I (^{11}C-PE2I) which showed favorable results (8, 9). However, there are potential limitations of ^{11}C-PE2I in quantifying DAT. Firstly, the relatively slow kinetics of ^{11}C-PE2I requires longer than 90 min imaging acquisitions. Secondly, a radiometabolite of ^{11}C-PE2I has been found to cross the blood-brain barrier (BBB) of rat brain, and accumulate in the striatum, which limited the kinetic analysis (10, 11). Also, relatively short half-life is an impediment of ^{11}C labeled compound for clinical application.

A fluoroethyl analogue of PE2I, [^{18}F]FE-PE2I (2-[^{18}F]Fluoroethyl 8-[(2E)-3-iodoprop-2-en-1-yl]-3-(4-methylphenyl)-8-azabicyclo[3.2.1]octane-2-

carboxylate) has been developed. In nonhuman primates, [^{18}F]FE-PE2I shows faster kinetics and less production of BBB-permeable radiometabolites. Also, binding potential (BP) could be reliably estimated by using simplified reference tissue model (SRTM) method with a 60-min image acquisition in human (12-15). In addition, considering longer half-life and lower positron energy of F-18 compared to C-11, F-18 labeled compound has advantage in dynamic PET experiment with higher spatial resolution. Therefore, [^{18}F]FE-PE2I could be used for DAT quantification as a PET radioligand. However, a limited number of study was published to validate the [^{18}F]FE-PE2I imaging in the PD model or patient (16).

The practical application of DAT imaging can be optimized when the binding of radioligands is robust when drugs are prescribed for the patients. Previous studies have shown that most of drugs, especially dopaminergic medication will not interfere the binding of various DAT radioligands in striatum (17-19). However, none of studies have assessed the effects of therapeutic drug on [^{18}F]FE-PE2I binding.

This study aimed to determine any correlation between striatal [^{18}F]FE-PE2I binding and immunohistochemical (IHC) stain for tyrosine hydroxylase (TH) of striatum. Also, the effects of therapeutic drug on [^{18}F]FE-PE2I binding were evaluated.

Materials and Methods

1. Animals

A total of 28 male Sprague-Dawley (SD) rats weighing 347.9 ± 17.9 g (mean±SD) at age of 10 weeks underwent [^{18}F]FE-PE2I PET/CT imaging. Eight rats were subjected to PD modeling 3 weeks before imaging. Among these rats, [^{18}F]FE-PE2I PET/CT imaging of 4 PD rats were compared with those of 4 normal rats. The remaining 4 PD rats underwent [^{18}F]FE-PE2I PET/CT twice, with placebo (normal saline) treatment or with L-DOPA/benserazide treatment, to compare the effects of L-DOPA/benserazide on striatal [^{18}F]FE-PE2I binding. Other drugs described below were tested on the normal rats to compare the effects of these drugs on [^{18}F]FE-PE2I binding.

This study was approved by the of Seoul National University Bundang hospital Institutional Review Board and Ethics Committee, and Institutional Animal Care and Use Committee.

2. Parkinson's disease modeling

Rats were anesthetized with an intraperitoneal injection of a combination of tiletamine/zolazepam (10 mg/kg; Zoletil 50, Virbac, Carros, France), and Xylazine HCl (10 mg/kg; Rumpen, Bayer Korea, Seoul, Korea) mixture, and placed

in a stereotaxic frame. The skull was exposed and a small hole was punctuated with the use of a bone drill. Then, each rat was injected with 20 μg of 6-OHDA (Sigma-Aldrich, St. Louis, MO, USA) dissolved in 4 μL of 0.05% ascorbic acid solution into the right striatum using Hamilton syringe at a flow rate of 0.5 μL/min (anteroposterior, 0.7 mm; mediolateral, -2.6 mm and dorsoventral, -4.5 mm from the bregma) (20, 21). Following the injection of 6-OHDA, the Hamilton syringe was sustained in place for 10 min to avoid backflow of 6-OHDA, and the incised scalp was sutured. After surgery, rats recovered from anesthesia in a temperature-controlled chamber before returning to the individual cages.

3. Drug Treatment

All drugs were purchased from Sigma (Sigma-Aldrich, St. Louis, MO), and dissolved in buffer solution at a volume of 1 mL/kg then administered 30 min before injection of [^{18}F]FE-PE2I. The dose of each drug for rat were determined by previous studies (22-25).

3.1. L-DOPA.

To investigate the effects of L-DOPA/benserazide on striatal [^{18}F]FE-PE2I binding, each of the 4 normal and PD rats were pretreated together with, 15 mg/kg of L-DOPA and benserazide at the dose ratio of 4:1 via intraperitoneal injection. Due to poor solubility, L-DOPA was initially dissolved in the 0.2 *M* HCL, neutralized with 7% $NaHCO_3$ and stabilized with 5% ascorbic acid (22). Striatal [^{18}F]FE-PE2I

bindings on 4 normal rats pretreated with L-DOPA/benserazide were compared with normal rats. Considering the effects of L-DOPA/benserazide on striatal [^{18}F]FE-PE2I binding according to DAT status, additional 4 PD rats were used. After 3 weeks of PD modeling, 4 PD rats underwent [^{18}F]FE-PE2I PET/CT with pretreatment of placebo (normal saline, i.p, 1 mL/kg) 30 min before imaging. After 24 hours, same rats underwent [^{18}F]FE-PE2I PET/CT with pretreatment of L-DOPA/benserazide.

3.2. Pramipexole

Rats were pretreated with 3 mg/kg of pramipexole, a DA agonist, dissolved in 0.9% NaCl via intraperitoneal injection.

3.3. Amantadine

Rats were pretreated with 40 mg/kg of amantadine, N-Methyl-D-aspartate (NMDA) receptor antagonist in 0.9% NaCl via intraperitoneal injection.

3.4. Escitalopram

Escitalopram, a selective serotonin reuptake inhibitor (SSRI) was administrated to assess the selectivity of [^{18}F]FE-PE2I binding to DAT. Escitalopram (5 mg/kg, i.p) was dissolved in 10% dimethyl sulfoxide.

4. Preparation of [^{18}F]FE-PE2I

[^{18}F]FE-PE2I was synthesized using conventional Kryptofix-mediated nucleophilic aliphatic ^{18}F-substitution on the tosylate leaving group of the precursor in TRACER lab FX N pro module (GE Healthcare) with a little modification according to literature (26). The non-decay corrected radiochemical yield for [^{18}F]FE-PE2I after HPLC purification and final formulation was 19.3 ± 2.1% (n = 42) with over 99% of radiochemical purity. The specific radioactivity was 792 ± 112 GBq/μmol at the time of end-of-synthesis (EOS). No significant radiolysis of [^{18}F]FE-PE2I was observed after 4 h at room temperature in a formulation containing 10% ethanol/PBS solution.

5. PET/CT Imaging

Before imaging, the rats were anesthetized with 5% isoflurane and sustained with 5% isoflurane in a 6:4 mixture of N_2/O_2. PET/CT imaging was performed in a dedicated small animal PET/CT (NanoPET/CT, Bioscan Inc., Washington DC, USA) with a 10 cm axial field of view (FOV) and a 12 cm transaxial FOV. Reconstructed PET spatial resolution was 1.2 mm full-width at half-maximum at the center of FOV. A CT scan of the head was used for attenuation correction. List-mode-data-based PET acquisition was concomitantly started with the intravenous injection of [^{18}F]FE-PE2I via tail vein. Dynamic PET/CT acquisition was performed for 90 min consisting of 54 frames of increasing duration, namely 12 at 10-seconds, 16 at 30-seconds, 8 at 1-minutes and 18 at 4-minutes. The acquired images were

reconstructed by a 3-D Adjoint Monte Carlo method with scatter and random corrections. Reconstructed voxel values in each frame are reported in units of kBq/cc, corrected for radioactive decay to the time of injection and the voxel dimensions were 0.8 X 0.8 X 0.8 mm^3. The voxel values were then converted to standardized uptake value (SUV) which calculated by kBq/cc divided by injection dose (kBq) per animal weight.

All drugs were administered 30 min via intraperitoneal injection before injection of [^{18}F]FE-PE2I. Dynamic PET acquisition was performed for 60 min consisting of 47 frames with increasing duration, namely 12 at 10-seconds, 16 at 30-seconds, 8 at 1-minutess and 11 at 4-minutes. The protocol for PET/CT acquisition and reconstruction were same as previous description.

6. Image Analysis

Analysis of the PET images was performed using PMOD software version 3.1 (PMOD Technologies Ltd., Zurich, Switzerland). All dynamic PET images were normalized to the standard space via co-registration to MRI rat brain template (20). For co-registration, dynamic PET images were first cropped to a manually drawn rectangular region containing the brain of rat. Next, the frames of the first 5 minutes after [^{18}F]FE-PE2I injection were averaged to create an early distribution image. This image was co-registered to MRI rat brain template by rigid transformation. This transformation was used to register all dynamic frames of PET images.

The volume of interest (VOIs) of the Schiffer template corresponding to the striatum, thalamus, midbrain and cerebellum were used to generate regional time-activity curves (TACs) on the co-registered images (27). For comparing the striatal [^{18}F]FE-PE2I binding in 6-OHDA treated rats and normal rats, the separate VOI was used on lesioned/unlesioned or contralateral/ipsilateral sides of striatum. Other striatal [^{18}F]FE-PE2I binding was assessed by the unified VOI for left and right sides. For thalamus and cerebellum, the left and right sides were included in the same VOI.

The correlation of striatal [^{18}F]FE-PE2I uptake and optical density (OD) of TH-reactive fiber were established by immunohistochemical stain, and average image from 5 min to 90 min were used to measure the ratio of lesioned and unlesioned sides of striatum.

7. Kinetic Analysis

Kinetic analysis was performed with SRTM method using the cerebellum as a reference region. This is an established method for quantification of DAT due to negligible DAT density in the cerebellum (7). Prior studies of [^{18}F]FE-PE2I in human and primate brain have also reported that BP could be reliably estimated from SRTM method (12,15).

SRTM method assumes that the level of nonspecific binding is the same in both target and reference regions, and that TAC of target and reference regions can be fit by a 1-tissue compartment model. According to this method, three unknown

parameters R_1, k_2 and BP_{ND} are fit using nonlinear regression method (28).

For investigating the applicability of shorter duration of image acquisition, BP_{ND} values with different imaging time from 90 to 30 min were compared.

8. Tissue Preparation and Immunohistochemistry

After [^{18}F]FE-PE2I PET/CT imaging, rats were sacrificed under anesthesia with isoflurane. Transcardiac perfusion with PBS was followed by 4% paraformaldehyde. Brains were removed and postfixed in 4% paraformaldehyde for 6 hours and 20% sucrose for overnight at 4℃, prior to sectioning on the microtome-cryostat (Microm HM 550 MP, UK). Six sections were obtained from each examined brain region and each section was 40 μm from the previous one. Free-floating sections were washed briefly with PBS 3 times and then endogenous peroxidase activity was suppressed by adding 3% H_2O_2. The sections were preincubated with 3% bovine serum albumin (BSA) and 0.1% Triton 100 in PBS for 30 min before transferring to anti-primary tyrosine hydroxylase (Millipore, USA, 1: 5000) in PBS containing 0.3% BSA and Trition X-100. Following incubation overnight at 4℃, the sections were incubated in a biotinylated anti-mouse immunoglobulin G (Vector laboratories, USA, 1:200) in PBS containing 0.3% BSA and Trition X-100 for 1 hour. The specimens were reincubated for 1 hour at room temperature with streptavidin–biotin–horseradish peroxidase complex (Vectastain, ABC kitElite, Vector Laboratories). TH immunoreactivity was visualized using 3, 3-diaminobenzidine

(DAB). Immunostained sections were mounted on glass slides and dehydrated in a solution of graded ethanol and Xylen. A fluorescence microscope (Axio Observer, Zeiss, Germany) with Image-Pro Plus 7.0 software (MediaCybernetics, Silver Spring, MD) and Image J software (National Institutes of Health, Bethesda, MD) was used to histologically quantify OD ratio of TH-reactive fibers in lesioned and unlesioned sides of striatum.

9. Statistical Analysis

All statistical analysis was performed using GraphPad Prism 5.0 software (GraphPad Software, Inc., San Diego, CA). Kruskal-Wallis test with Dunn's multiple comparison test for post-hoc analysis was performed to compare the difference of BP_{ND} of PD and normal rat, and to assess the effects of therapeutic drugs on [^{18}F]FE-PE2I binding. In the additional experiment of assessing the L-DOPA/benserazide on 4 PD rats, the differences of BP_{ND} in each striatum were analyzed by Wilcoxon signed rank test. For assessing the correlation between OD of TH-reactive fibers and [^{18}F]FE-PE2I binding in the striatum, and between lesioned and unlesioned striatal BP_{ND} on 8 PD rats, Spearman's non-parametric correlation (rho, r) was used. In all statistical analyses, P value < 0.05 was considered significant.

Results

1. [^{18}F]FE-PE2I for DAT imaging in rat brain

1.1 Regional Brain Uptake

Representative PET images and TACs for [^{18}F]FE-PE2I on normal rats are shown in Figure 1 and Figure 2A. [^{18}F]FE-PE2I showed high accumulation in the striatum with low uptake in the midbrain. Accumulation of radioactivity in striatum peaked at 2.5 min after injection and followed by a continuous washout of radioactivity to a level of 0.32 SUV at 90 min. The cerebellum peaked at 50 sec and decreased to a stable level of 0.30 SUV at 42 min. The ratio of uptake in the striatum and midbrain to cerebellum was 1.1-2.5 and 0.9-1.4 respectively. BP_{ND} measured with SRTM method was 1.1 in the striatum and 0.25 in the midbrain.

Figure 2B shows the TAC for [^{18}F]FE-PE2I on PD rats. Lesioned striatal TAC was lower than unlesioned one. Also, midbrain TAC was lower than cerebellar TAC after 24min post injection. BP_{ND} was significantly lower in the lesioned striatum than in the unlesioned one or the striatum of normal rats ($P < 0.05$ according to Dunn's multiple comparison test) (Fig 3). There was a tendency that BP_{ND} of unlesioned striatum from PD rats were lower than that from normal rats, however, it does not reach significance. Midbrain BP_{ND} of PD rats was significantly lower than that of normal rats (<0.01 vs 0.25, $P < 0.05$ according to Kruskal-Wallis test). Representative coronal and transaxial PET images of BP_{ND} parametric map of [^{18}F]FE-PE2I and TH staining coronal section are shown in Figure 4.

From total 8 PD rats, there was a significant correlation between lesioned and unlesioned striatal BP_{ND} (n=8, Spearman's non-parametric correlation test; r=0.738, $P<0.05$) (Fig 5).

There was a linear correlation between the ratio of OD of TH-reactive fibers and the ratio of [^{18}F]FE-PE2I binding in the striatum (n=8, Spearman's non-parametric correlation test; r=0.741, $P<0.05$).

1.2 Imaging Time Dependency of Striatal BP_{ND}

The values of striatal BP_{ND} were relatively stable in relation to the imaging time of 60 min to 90 min (Fig 6). With a 60-min imaging time, BP_{ND} of striatum were approximately 103% of that of a 90-min imaging time.

2. Therapeutic Drug Effects on [^{18}F]FE-PE2I Binding

Figure 7 shows the striatal BP_{ND} after administration of all therapeutic drugs under study. After pre-treatment of pramipexole, amantadine and escitalopram, the values of striatal [^{18}F]FE-PE2I binding did not differ from those of control rats. However, pre-treatment of L-DOPA/benserazide significantly reduced the striatal BP_{ND} ($P = 0.03$ according to Dunn's multiple comparison test).

For midbrain [^{18}F]FE-PE2I binding, there was no significant difference between control rats and escitalopram treated one (0.25 vs 0.23, $P > 0.05$ according to Dunn's multiple comparison test).

As discussed below, considering the possible L-DOPA/benserazide effects on [^{18}F]FE-PE2I binding according to the status of DAT expression, additional experiments were performed using PD rats. Each striatal BP_{ND} (lesioned and unlesioned striatum) were compared with placebo (normal saline) and L-DOPA/benserazide treatment. There was no statistical significant difference of striatal BP_{ND} between placebo and L-DOPA/benserazide treatment in both lesioned and unlesioned striatum of PD rats ($P>0.05$ according to Wilcoxon signed rank test).

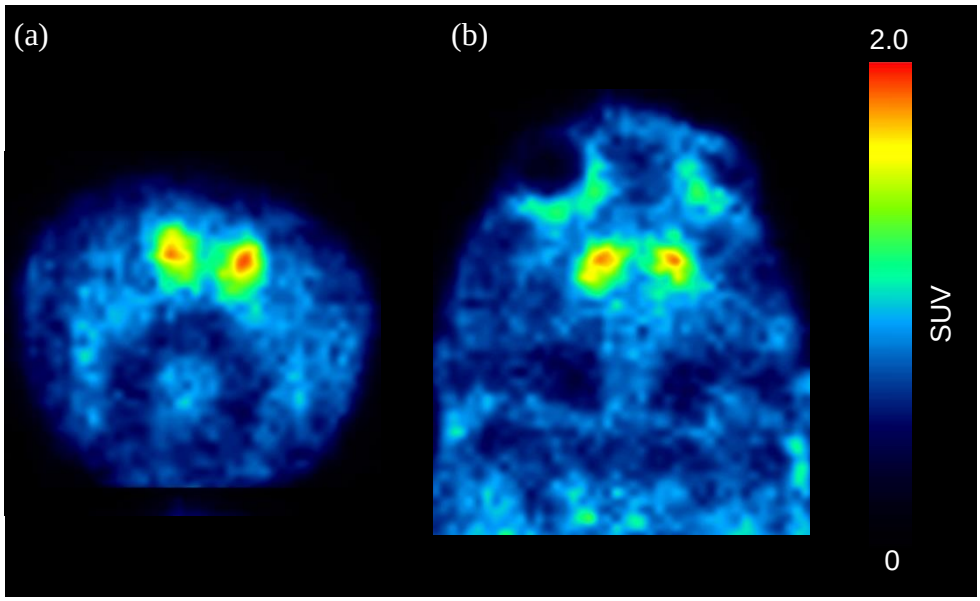

Figure 1. (a) Coronal and (b) transaxial average PET image from 5min to 90 min after IV injection of [^{18}F]FE-PE2I in rat number 3.

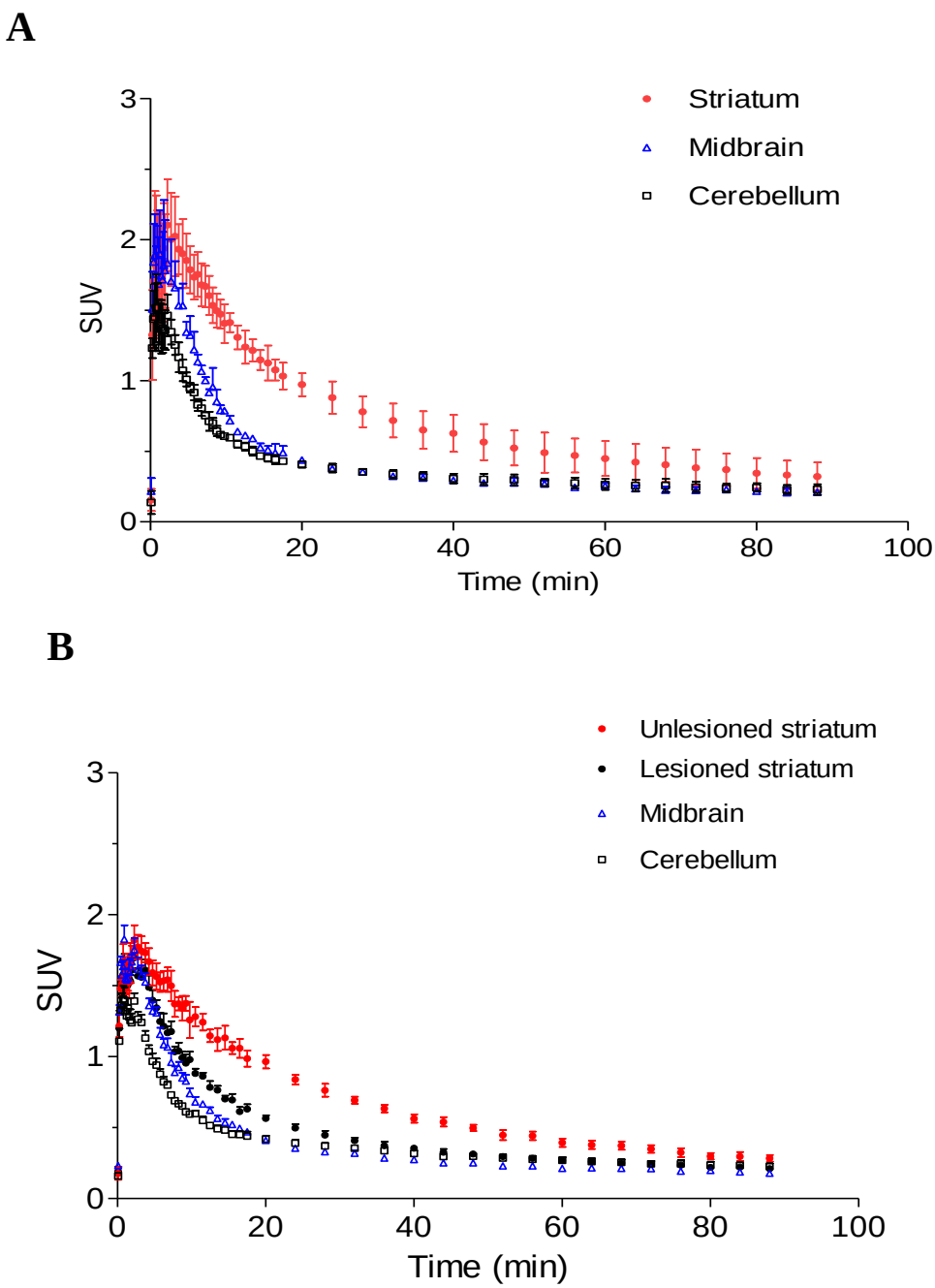

Figure 2. TACs for regional brain uptake after IV injection of [^{18}F]FE-PE2I (A) on normal rats (B) on PD rats. Data represent mean ± standard error (SE) (n = 4).

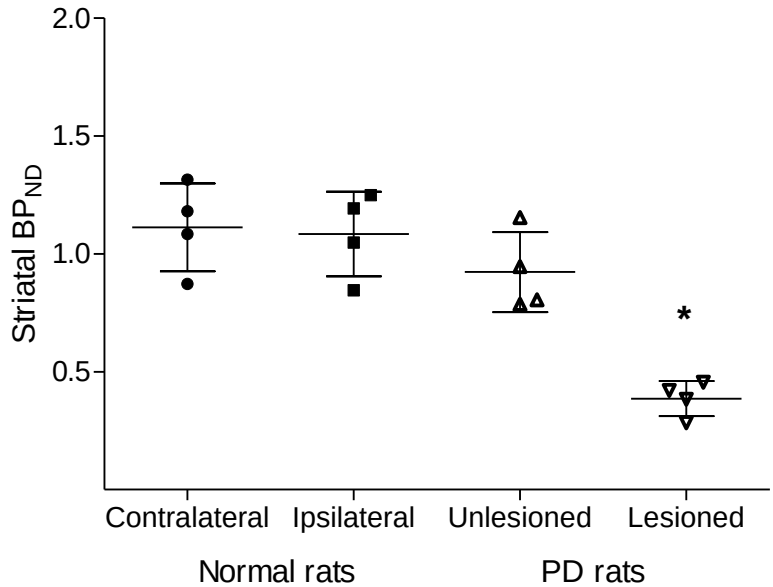

Figure 3. Comparison of striatal BP_{ND} between normal and PD rats. (n = 4 each, * for $P<0.05$ according to Dunn's multiple comparison test)

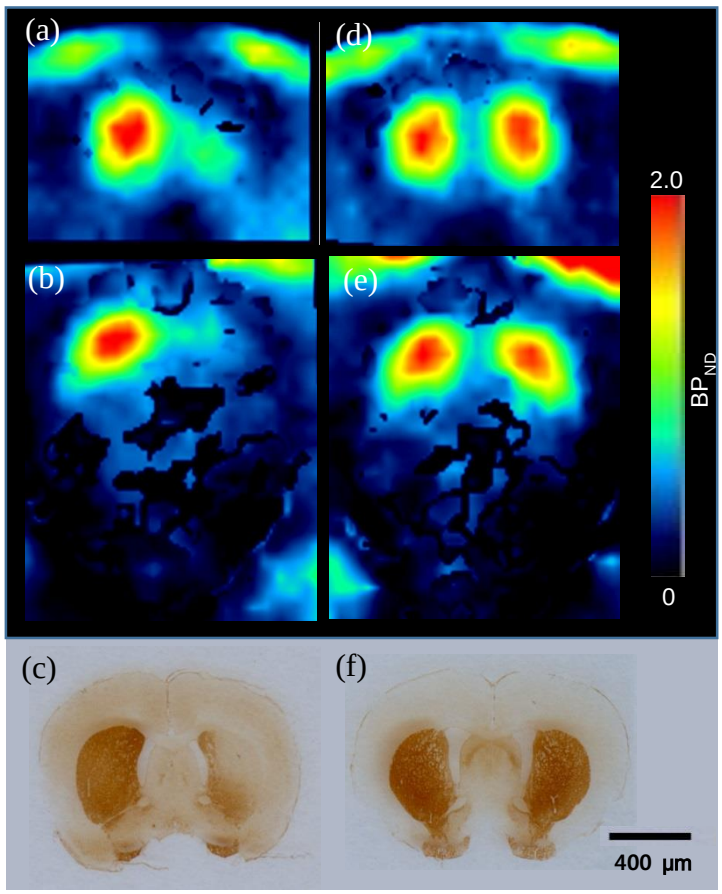

Figure 4. Representative BP_{ND} parametric map of [^{18}F]FE-PE2I and TH staining section. (a) Coronal, (b) transaxial image of BP_{ND} parametric map, and (c) TH staining coronal section for PD rat. (d) - (f) for normal rat.

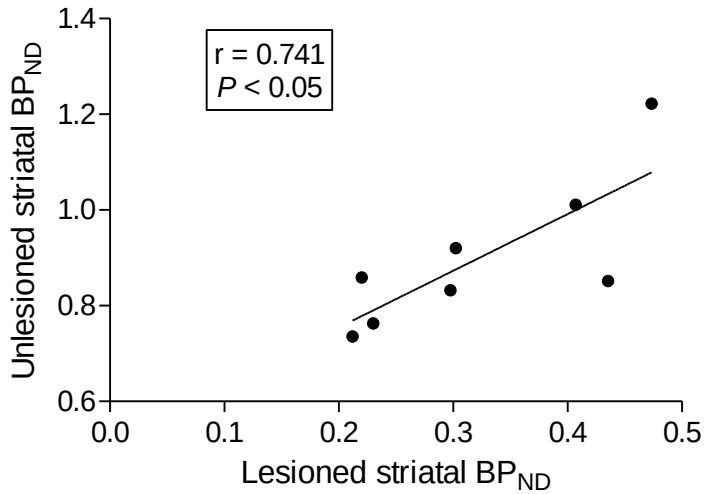

Figure 5. Correlation between lesioned and unlesioned striatal BP_{ND} of PD rats (n=8).

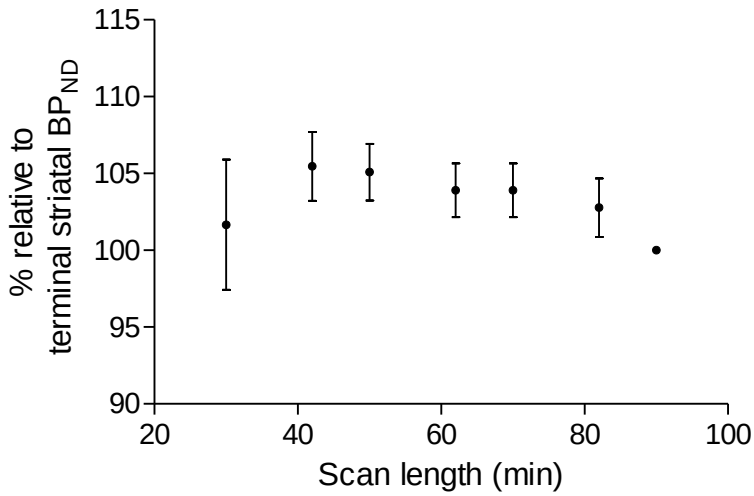

Figure 6. Time dependency of striatal BP_{ND} as a function of duration of PET measurement on normal rat. Striatal BP_{ND} values are expressed as percentage of terminal value. Error bar represents SE (n=4).

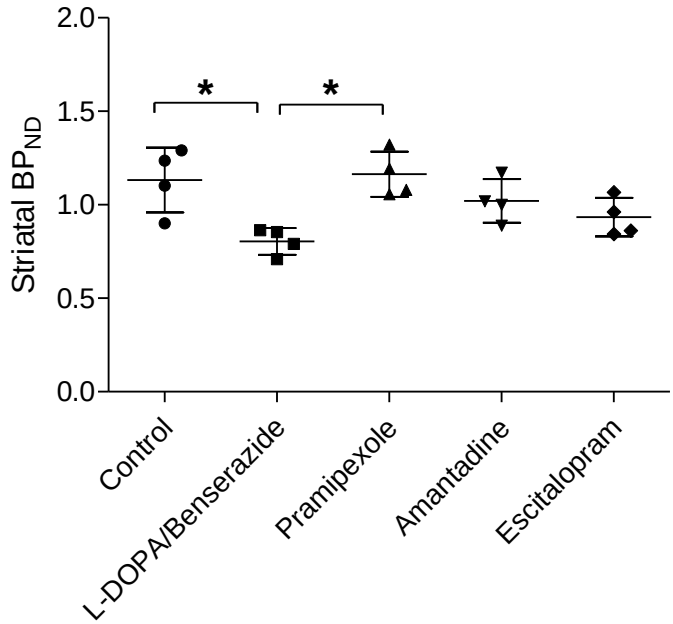

Figure 7. Striatal BP_{ND} of [^{18}F]FE-PE2I after pre-treated each drugs. (n = 4 each, * for $P < 0.05$ according to Dunn's multiple comparison test).

Discussion

1. [^{18}F]FE-PE2I for DAT Imaging in Rat Brain

PE2I has been known as a potent radioligand for DAT imaging with high affinity and selectivity, with various isotopes such as ^{123}I, ^{3}H or ^{11}C (6). ^{11}C-PE2I has been established to provide high-resolution PET image of DAT including human studies, however limited clinical application due to slow kinetic properties, and production of BBB-permeable radiometabolites (10, 11). Recently [^{18}F]FE-PE2I has been developed, and showed relatively fast kinetics and favorable metabolism that could be reliable for DAT quantification (12-15). The presented study demonstrated the fast kinetics of [^{18}F]FE-PE2I in the rat brain. The result of stability of BP_{ND} according to the shorter imaging time, 60 min would be adequate to obtain reliable estimate of [^{18}F]FE-PE2I binding. Excellent correlation between [^{18}F]FE-PE2I binding ratios was measured in vivo by PET, and the striatal TH concentration measured IHC stain, which signifies the dopaminergic cell loss. From data gathered, [^{18}F]FE-PE2I could be used as a radioligand for in vivo imaging of the DAT and quantification.

The striatal uptake of [^{18}F]FE-PE2I in rat brain were lower than that of ^{11}C-PE2I in rat brain which were established in previous studies (11). Although there was no previous studies using rat brain for [^{18}F]FE-PE2I imaging, there is a

consensus of lower BP value in [^{18}F]FE-PE2I compared with ^{11}C-PE2I on human and nonhuman primate studies (12, 14, 15, 29-31). Considering that in vitro DAT binding affinity of PE2I and [^{18}F]FE-PE2I is almost identical (K_i value for DAT 17nM vs. 12nM for PE2I and [^{18}F]FE-PE2I, respectively), adding the fluoroethyl group in the ester moiety of PE2I could change the in vivo DAT binding kinetics and may varies between animal used for [^{18}F]FE-PE2I imaging.

DAT is also known to localize in the midbrain, which contains dopaminergic cell bodies. Reduced DAT on midbrain accompanies the neurodegeneration of midbrain dopaminergic neurons on PD (32, 33). However, midbrain uptake of previous DAT tracers such as FP-CIT or β-CIT was considered to bind on SERT due to the relatively high affinity to monoamine transporters. Also, pre-treated SSRI significantly reduced those binding on midbrain (34-36). From the presented study, [^{18}F]FE-PE2I binding on midbrain was significantly decreased on PD rats compared to normal rats. Pre-treatment of SSRI did not influence the midbrain BP_{ND}, therefore those results might represent the selectivity of [^{18}F]FE-PE2I binding on DAT especially midbrain.

2. Therapeutic Drug Effects on [^{18}F]FE-PE2I Binding

The study showed that the specific binding of [^{18}F]FE-PE2I on the striatum was not influenced by the DA receptor agonist and NMDA receptor antagonist,

which drugs are conventionally used in treatment PD patients. Also, the results that pretreated SSRI before imaging did not affect the striatal [^{18}F]FE-PE2I binding.

The effects of pretreated L-DOPA/benserazide on the striatal [^{18}F]FE-PE2I binding is interesting. There were several studies to investigate the effect of L-DOPA in DAT imaging on animals and human, which reported controversial results; acute intraperitoneal administration of various doses of L-DOPA (5 mg/kg, 10 mg/kg, 125 and 150 mg/kg, i.p injection) or long-term treatment of 10 mg/kg L-DOPA (i.p injection) with or without DOPA decarboxylase inhibitor in healthy rats induced the reduction of DAT binding (37-39). In contrast to this, acute or subacute oral administration of 100 mg/kg of L-DOPA in healthy rats had no influence on DAT binding (40). Interestingly, Sossi *et al.* assessed the chronic L-DOPA treated effect on DAT binding using unilaterally 6-OHDA lesioned rats and showed that denervation-dependent increase of DAT binding (39). For animal studies, the results might be affected by the methodologies such as dose of L-DOPA, administration route, administration period and DAT expression status. Whereas, in nonhuman primates and human studies, L-DOPA does not affect the DAT binding (17-19). In conclusion, L-DOPA effect on DAT binding are unpredictable.

In our study, the dose of L-DOPA/benserazide was chosen as therapeutic range for rat (22). Although L-DOPA/benserazide is prescribed for oral intake in clinical practice, for the consistency of bioavailability among the rats, intraperitoneal administration was chosen. The results show that acute administration of 15 mg/kg L-DOPA with benserazide (i.p injection) on normal rats induced significant reduction of DAT binding, but not on PD rats. As L-DOPA acts on the release of

endogenous DA, in normal striatum, the reduction of DAT binding might be due to the competition between [^{18}F]FE-PE2I and endogenous DA (41). In PD rats, decreased capacity of synthesizing and releasing endogenous DA could account for the [^{18}F]FE-PE2I DAT binding of lesioned striatum which was not affected by L-DOPA administration.

DAT binding of [^{18}F]FE-PE2I on unlesioned striatum of PD rats was not affected by L-DOPA/benserazide contrary to the normal striatum. Considering that there have been reports of the possible inter-hemispheric compensatory reaction in unilateral PD model animals and crossed nigrostriatal pathway in rats, comparison between normal striatum of normal rats and unlesioned striatum of PD rat might not be possible. (42-44). In our study, although there is no statistical significance, there was a tendency of lower values of BP_{ND} in the unlesioned striatum of PD rats compared to that of normal rats. Also, giving rise to a correlation between the lesioned and unlesioned striatal BP_{ND} of PD rats, there might be an unknown pathophysiology between the lesioned to that of the unlesioned striatum with or without L-DOPA treatment. Nevertheless, L-DOPA/benserazide did not affect the DAT binding of [^{18}F]FE-PE2I on unlesioned striatum of PD rats.

There are potential limitations regarding the methodology of our study. The number of rats we used might be insufficient to assess the effects of therapeutic drugs on striatal $BP_{ND.}$ Additional experiment with L-DOPA/benserazide treatment was conducted by paired study design to prove the drug effect deducing the individual difference. Another limitation is that we did not perform sham operation of normal rats in comparing with unilateral 6-OHDA PD rats. The intrastriatal injection is a

well-established method (45) and the time interval between the modeling and the imaging acquisition was sufficient to reduce the possible influence. Therefore, omitting the sham operation might reduce the number of animals used as possible. Also, evaluation of midbrain in rat brain from PET image would be limited due to partial volume effect. Lastly, there is a possibility of isoflurane to change the DAT expression, but not examined in our animal models (46, 47).

For assessing the effects of typical therapeutic drugs for PD on striatal binding of [^{18}F]FE-PE2I, we used the unilateral 6-OHDA rats model. However, due to the complexity of pathophysiology of PD and limitation of PD animal models, further study of drugs effect are necessary on human. Long-term usage of these drugs should also validate the [^{18}F]FE-PE2I as a DAT imaging.

Conclusion

Our study shows that [^{18}F]FE-PE2I is a promising radioligand for in vivo imaging of the DAT. [^{18}F]FE-PE2I binding is unaffected by acute administration of typical therapeutic drugs for PD including DA receptor agonist, NMDA receptor antagonist and SSRI on normal striatum. Acute administration of L-DOPA/benserazide does not affect the [^{18}F]FE-PE2I binding on PD rat as supported by our study. Additional study is needed on human and with long-term treatment neuropsychiatric medications.

Reference

1. Shih MC, Hoexter MQ, Andrade LAFd, Bressan RA. Parkinson s disease and dopamine transporter neuroimaging: a critical review. Sao Paulo Medical Journal. 2006;124(3):168-75.

2. Spencer TJ, Biederman J, Madras BK, Dougherty DD, Bonab AA, Livni E, et al. Further evidence of dopamine transporter dysregulation in ADHD: a controlled PET imaging study using altropane. Biological psychiatry. 2007;62(9):1059-61.

3. Seeman P, Niznik HB. Dopamine receptors and transporters in Parkinson's disease and schizophrenia. The FASEB Journal. 1990;4(10):2737-44.

4. Lang AE, Lozano AM. Parkinson's disease. New England Journal of Medicine. 1998;339(15):1044-53.

5. Ginovart N, Lundin A, Farde L, Halldin C, Bäckman L, Swahn C-G, et al. PET study of the pre-and post-synaptic dopaminergic markers for the neurodegenerative process in Huntington's disease. Brain. 1997;120(3):503-14.

6. Emond P, Guilloteau D, Chalon S. PE2I: a radiopharmaceutical for in vivo exploration of the dopamine transporter. CNS neuroscience & therapeutics. 2008;14(1):47-64.

7. Hall H, Halldin C, Guilloteau D, Chalon S, Emond P, Besnard J-C, et al. Visualization of the Dopamine Transporter in the Human Brain Postmortem with the New Selective Ligand [125I] PE2I. Neuroimage. 1999;9(1):108-16.

8. Dolle F, Bottlaender M, Demphel S, Emond P, Fuseau C, Coulon C, et al. Highly efficient synthesis of [11C] PE2I, a selective radioligand for the quantification of the dopamine transporter using PET. Journal of Labelled Compounds and Radiopharmaceuticals. 2000;43(10):997-1004.

9. Halldin C, Erixon-Lindroth N, Pauli S, Chou Y-H, Okubo Y, Karlsson P, et al. [11C] PE2I: a highly selective radioligand for PET examination of the dopamine transporter in monkey and human brain. European journal of nuclear medicine and molecular imaging. 2003;30(9):1220-30.

10. Hirvonen J, Johansson J, Teräs M, Oikonen V, Lumme V, Virsu P, et al. Measurement of striatal and extrastriatal dopamine transporter binding with high-resolution PET and 11C PE2I: quantitative modeling and test–retest reproducibility. Journal of Cerebral Blood Flow & Metabolism. 2008;28(5):1059-69.

11. Shetty HU, Zoghbi SS, Liow J-S, Ichise M, Hong J, Musachio JL, et al. Identification and regional distribution in rat brain of radiometabolites of the dopamine transporter PET radioligand [11C] PE2I. European journal of

nuclear medicine and molecular imaging. 2007;34(5):667-78.

12. Sasaki T, Ito H, Kimura Y, Arakawa R, Takano H, Seki C, et al. Quantification of dopamine transporter in human brain using PET with 18F-FE-PE2I. Journal of Nuclear Medicine. 2012;53(7):1065-73.

13. Varrone A, Gulyás B, Takano A, Stabin MG, Jonsson C, Halldin C. Simplified quantification and whole-body distribution of [18F] FE-PE2I in nonhuman primates: prediction for human studies. Nuclear medicine and biology. 2012;39(2):295-303.

14. Varrone A, Steiger C, Schou M, Takano A, Finnema SJ, Guilloteau D, et al. In vitro autoradiography and in vivo evaluation in cynomolgus monkey of [18F] FE-PE2I, a new dopamine transporter PET radioligand. Synapse. 2009;63(10):871-80.

15. Varrone A, Tóth M, Steiger C, Takano A, Guilloteau D, Ichise M, et al. Kinetic analysis and quantification of the dopamine transporter in the nonhuman primate brain with 11C-PE2I and 18F-FE-PE2I. Journal of Nuclear Medicine. 2011;52(1):132-9.

16. Fazio P, Svenningsson P, Forsberg A, Jonsson EG, Amini N, Nakao R, et al. Quantitative Analysis of 18F-(E)-N-(3-Iodoprop-2-Enyl)-2beta-Carbofluoroethoxy-3beta-(4'-Methyl-Phenyl) Nortropane Binding to the Dopamine Transporter in Parkinson Disease. Journal of nuclear medicine : official publication, Society of Nuclear Medicine. 2015;56(5):714-20.

17. Fernagut PO, Li Q, Dovero S, Chan P, Wu T, Ravenscroft P, et al. Dopamine transporter binding is unaffected by L-DOPA administration in normal and MPTP-treated monkeys. PloS one. 2010;5(11):e14053.

18. Innis RB, Marek KL, Sheff K, Zoghbi S, Castronuovo J, Feigin A, et al. Effect of treatment with L-dopa/carbidopa or L-selegiline on striatal dopamine transporter SPECT imaging with [123I]beta-CIT. Movement disorders : official journal of the Movement Disorder Society. 1999;14(3):436-42.

19. Schillaci O, Pierantozzi M, Filippi L, Manni C, Brusa L, Danieli R, et al. The effect of levodopa therapy on dopamine transporter SPECT imaging with(123)I-FP-CIT in patients with Parkinson's disease. Eur J Nucl Med Mol Imaging. 2005;32(12):1452-6.

20. Paxinos G, Watson C. The rat brain in stereotaxic coordinates: Academic press; 2006.

21. Perumal AS, Tordzro WK, Katz M, Jackson-Lewis V, Cooper TB, Fahn S, et al. Regional effects of 6-hydroxydopamine (6-OHDA) on free radical scavengers in rat brain. Brain research. 1989;504(1):139-41.

22. Bredberg E, Lennernäs H, Paalzow L. Pharmacokinetics of levodopa and carbidopa in rats following different routes of administration. Pharmaceutical research. 1994;11(4):549-55.

23. Montgomery SA, Loft H, Sánchez C, Reines EH, Papp M.

Escitalopram (S-Enantiomer of Citalopram): Clinical Efficacy and Onset of Action Predicted from a Rat Model. Pharmacology & toxicology. 2001;88(5):282-6.

24. Page G, Peeters M, Maloteaux J-M, Hermans E. Increased dopamine uptake in striatal synaptosomes after treatment of rats with amantadine. European journal of pharmacology. 2000;403(1):75-80.

25. Vu T, Ling Z, Ma S, Robie H, Tong C, Chen E, et al. Pramipexole attenuates the dopaminergic cell loss induced by intraventricular 6-hydroxydopamine. Journal of neural transmission. 2000;107(2):159-76.

26. Stepanov V, Krasikova R, Raus L, Loog O, Hiltunen J, Halldin C. An efficient one-step radiosynthesis of [18F] FE-PE2I, a PET radioligand for imaging of dopamine transporters. Journal of Labelled Compounds and Radiopharmaceuticals. 2012;55(6):206-10.

27. Schiffer WK, Mirrione MM, Dewey SL. Optimizing experimental protocols for quantitative behavioral imaging with 18F-FDG in rodents. Journal of Nuclear Medicine. 2007;48(2):277-87.

28. Lammertsma AA, Hume SP. Simplified reference tissue model for PET receptor studies. Neuroimage. 1996;4(3):153-8.

29. DeLorenzo C, Kumar JD, Zanderigo F, Mann JJ, Parsey RV. Modeling considerations for in vivo quantification of the dopamine transporter using 11C PE2I and positron emission tomography. Journal of

Cerebral Blood Flow & Metabolism. 2009;29(7):1332-45.

30. Jucaite A, Odano I, Olsson H, Pauli S, Halldin C, Farde L. Quantitative analyses of regional [11C] PE2I binding to the dopamine transporter in the human brain: a PET study. European journal of nuclear medicine and molecular imaging. 2006;33(6):657-68.

31. Seki C, Ito H, Ichimiya T, Arakawa R, Ikoma Y, Shidahara M, et al. Quantitative analysis of dopamine transporters in human brain using [11C] PE2I and positron emission tomography: evaluation of reference tissue models. Annals of nuclear medicine. 2010;24(4):249-60.

32. Frost JJ, Rosier AJ, Reich SG, Smith JS, Ehlers MD, Snyder SH, et al. Positron emission tomographic imaging of the dopamine transporter with 11C-WIN 35,428 reveals marked declines in mild Parkinson's disease. Ann Neurol. 1993;34(3):423-31.

33. Uhl GR, Walther D, Mash D, Faucheux B, Javoy-Agid F. Dopamine transporter messenger RNA in Parkinson's disease and control substantia nigra neurons. Annals of neurology. 1994;35(4):494-8.

34. Booij J, de Jong J, de Bruin K, Knol R, de Win MM, van Eck-Smit BL. Quantification of striatal dopamine transporters with 123I-FP-CIT SPECT is influenced by the selective serotonin reuptake inhibitor paroxetine: a double-blind, placebo-controlled, crossover study in healthy control subjects. Journal of nuclear medicine : official publication, Society of Nuclear

Medicine. 2007;48(3):359-66.

35. de Win MM, Habraken JB, Reneman L, van den Brink W, den Heeten GJ, Booij J. Validation of [(123)I]beta-CIT SPECT to assess serotonin transporters in vivo in humans: a double-blind, placebo-controlled, crossover study with the selective serotonin reuptake inhibitor citalopram. Neuropsychopharmacology : official publication of the American College of Neuropsychopharmacology. 2005;30(5):996-1005.

36. Laruelle M, Baldwin RM, Malison RT, Zea-Ponce Y, Zoghbi SS, al-Tikriti MS, et al. SPECT imaging of dopamine and serotonin transporters with [123I]beta-CIT: pharmacological characterization of brain uptake in nonhuman primates. Synapse. 1993;13(4):295-309.

37. Nikolaus S, Beu M, Hautzel H, Silva AM, Antke C, Wirrwar A, et al. Effects of L-DOPA on striatal iodine-123-FP-CIT binding and behavioral parameters in the rat. Nuclear medicine communications. 2013;34(12):1223-32.

38. Dresel SH, Kung MP, Plossl K, Meegalla SK, Kung HF. Pharmacological effects of dopaminergic drugs on in vivo binding of [99mTc]TRODAT-1 to the central dopamine transporters in rats. European journal of nuclear medicine. 1998;25(1):31-9.

39. Sossi V, Dinelle K, Schulzer M, Mak E, Doudet DJ, de la Fuente-Fernandez R. Levodopa and pramipexole effects on presynaptic dopamine

PET markers and estimated dopamine release. Eur J Nucl Med Mol Imaging. 2010;37(12):2364-70.

40. Lavalaye J, Knol RJ, de Bruin K, Reneman L, Janssen AG, Booij J. [123I]FP-CIT binding in rat brain after acute and sub-chronic administration of dopaminergic medication. European journal of nuclear medicine. 2000;27(3):346-9.

41. Misu Y, Goshima Y, Kubo T. Biphasic actions of L-DOPA on the release of endogenous dopamine via presynaptic receptors in rat striatal slices. Neuroscience letters. 1986;72(2):194-8.

42. Blesa J, Juri C, Garcia-Cabezas MA, Adanez R, Sanchez-Gonzalez MA, Cavada C, et al. Inter-hemispheric asymmetry of nigrostriatal dopaminergic lesion: a possible compensatory mechanism in Parkinson's disease. Frontiers in systems neuroscience. 2011;5:92.

43. Fass B, Butcher LL. Evidence for a crossed nigrostriatal pathway in rats. Neuroscience letters. 1981;22(2):109-13.

44. Narang N, Hunt ME, Pundt LL, Alburges ME, Wamsley JK. Unilateral ibotenic acid lesion of the caudate putamen results in D2 receptor alterations on the contralateral side. Experimental neurology. 1993;121(1):40-7.

45. Khan MM, Ahmad A, Ishrat T, Khan MB, Hoda MN, Khuwaja G, et al. Resveratrol attenuates 6-hydroxydopamine-induced oxidative damage and

dopamine depletion in rat model of Parkinson's disease. Brain Res. 2010;1328:139-51.

46. Fink-Jensen A, Ingwersen SH, Nielsen PG, Hansen L, Nielsen EB, Hansen AJ. Halothane anesthesia enhances the effect of dopamine uptake inhibition on interstitial levels of striatal dopamine. Naunyn-Schmiedeberg's archives of pharmacology. 1994;350(3):239-44.

47. Votaw JR, Byas-Smith MG, Voll R, Halkar R, Goodman MM. Isoflurane alters the amount of dopamine transporter expressed on the plasma membrane in humans. Anesthesiology. 2004;101(5):1128-35.

국문 초록

항파킨슨병 약물이 도파민 운반체 PET 방사성 추적자 [^{18}F]FE-PE2I의 도파민 운반체 결합에 미치는 영향

서울대학교 대학원

의학과 뇌신경과학 전공

방 지 인

목적:

[^{18}F]FE-PE2I는 도파민 운반체를 영상화 할 수 있는 방사성추적자이다. 본 연구에서는 파킨슨병 모델의 소동물 쥐를 이용하여 [^{18}F]FE-PE2I의 정량 분석을 시행하고, 선조체 조직의 tyrosine hydroxylase(TH)에 대한 면역화학염색을 통하여 선조체의 [^{18}F]FE-PE2I 축적과의 연관성을 평가하고자 한다. 또한 선조체의 [^{18}F]FE-PE2I 축적에 대하여 항파킨슨병의 치료약제에 의한 영향에 대하여 평가하고자 한다.

방법:

6-OHDA를 한쪽 선조체에 주입하여 파킨슨병 모델 쥐를 만들고, [^{18}F]FE-PE2I를 주사하여 dynamic PET/CT를 촬영하였다. 소뇌를 reference로 하여, simplified reference tissue model method을 통한 선조체 binding potential (striatal BP_{ND})을 구하였다. 파킨슨병 모델 쥐와 정상 쥐에서, TH 면역화학염색이 된 조직의 optical density(OD)를 구하여 striatal BP_{ND} 과의 연관성을 살펴보았다. 치료 약제에 대한 영향을 평가하기 위하여, 각 약물별 정상 쥐 4마리에 대하여, L-DOPA와 benserazide의 혼합 (L-DOPA/benserazide), pramipexole, amantadine, escitalopram을 [^{18}F]FE-PE2I 주입 30분 전에 투여하고, 약물을 투여하지 않은 대조군과 striatal BP_{ND}을 비교하였다. 또한, L-DOPA/benserazide 투여에 대해서는, 파킨슨병 모델 쥐 4마리를 추가적으로 사용하였다.

결과:

파킨슨병 모델 쥐의 모델링한 선조체의 BP_{ND}는 모델링하지 않은 반대쪽 선조체 혹은 정상 쥐의 선조체의 BP_{ND}와 비교하여 유의하게 낮았다. TH 면역화학염색이 된 조직의 OD ratio는 BP_{ND} ratio와 유의한 상관관계를 나타냈다 ($r=0.741$, $P<0.05$). Pramipexole, amantadine, escitalopram을 투여하였을 때, striatal BP_{ND} 는 대조군과 비교하여 유의한 차이가 없었다. L-DOPA/benserazide를 투여한 경우 striatal BP_{ND}가 대조군에 비교하여 유의하게 낮았다 ($P=0.03$). 그러나 파킨슨병 모델 쥐에서 L-DOPA/benserazide를 경우 같은 쥐에서 플라시보(생리식염수)와 비교하였을 때 유의한 차이를 보이지 않았다.

결론:

[^{18}F]FE-PE2I는 도파민 운반체를 생체 내에서 영상화하는데 사용할 수 있는 유용한 방사성추적자로서, [^{18}F]FE-PE2I 영상화에 있어서, 정상 쥐에서는 파킨슨병 환자에서 사용하는 약물인 Pramipexole, amantadine, escitalopram에 영향을 받지 않았다. 파킨슨병 모델 쥐에서의 L-DOPA/benserazide의 투여 또한 [^{18}F]FE-PEI의 선조체 결합에 영향을 주지 않았다.

중심단어: 파킨슨병, 도파민 트랜스포터, (E)-N-(3-iodoprop-2-enyl)-2beta-carbofluoroethoxy-3beta-(4'-methyl-phenyl) nortropane, 레보도파, 양전자단층촬영

학번: 2013-23506